Comparison of Theoretical and Flight-Measured Local Flow Aerodynamics for a Low-Aspect-Ratio Fin

J. Blair Johnson and Doral R. Sandlin

December 1986

Comparison of Theoretical and Flight-Measured Local Flow Aerodynamics for a Low-Aspect-Ratio Fin

J. Blair Johnson
Ames Research Center, Dryden Flight Research Facility, Edwards, California

Doral R. Sandlin
California Polytechnic State University, San Luis Obispo, California

1986

SUMMARY

Flight test and theoretical aerodynamic data were obtained for a flight test
fixture mounted on the underside of an F-104G aircraft. The theoretical data were
generated using two codes: (1) a two-dimensional transonic code called code H, and
(2) a three-dimensional subsonic and supersonic code called wing-body. Pressure
distributions generated by the codes for the flight test fixture, as well as
boundary-layer displacement thickness generated by the two-dimensional code, were
compared with the flight-measured data. The two-dimensional code pressure distri-
butions compared well except at the minimum pressure point and the trailing edge.
Shock locations compared well except at high transonic speeds. However, the two-
dimensional code did not adequately predict the displacement thickness of the
flight test fixture. The three-dimensional code pressure distributions compared
well except at the trailing edge of the flight test fixture.

INTRODUCTION

The use of theoretical prediction techniques can be a useful tool in most engi-
neering applications. In the case of aerodynamics, many computer codes exist that
aid the engineer with the design and analysis of aircraft and aircraft components.
Two commonly used codes are a two-dimensional transonic analysis code developed by
Bauer, Garabedian, Korn, and Jameson (ref. 1), and a three-dimensional subsonic and
supersonic wing-body analysis code developed by Woodward (ref. 2). Both analysis
codes have been used successfully in predicting parameters for specific shapes.
For example, the two-dimensional code, hereafter referred to as code H, has been
used successfully for the prediction of supercritical airfoil characteristics; the
three-dimensional code, hereafter referred to as the wing-body code, has been used
successfully to predict the characteristics of various wing-fuselage configurations.

Wind tunnel tests are frequently used as a means of obtaining experimental data.
However, such data usually must be corrected to obtain results that are valid for
flight vehicles. When conducting wind tunnel tests, consideration must be given to
limitations such as scale effects due to Reynolds number, size limitations for
models or test specimens due to test section dimension, and improper scaling of
noise or turbulence levels in the wind tunnel. Unreliable data near Mach 1 due to
problems such as shock reflections off of the tunnel walls must also be considered.
The Dryden Flight Research Facility of NASA Ames Research Center (Ames-Dryden) has
developed an instrumented flight test fixture (FTF) that can be attached to the
underside of an F-104G aircraft and used as a "flying wind tunnel." The FTF is
essentially a low-aspect-ratio fin incorporating a wedge-shaped airfoil.

A need exists (1) to verify that code H will accurately predict the aerodynamic
parameters for shapes other than those for which it was developed, and (2) to find
an aerodynamic code that will predict the aerodynamic parameters for the shape used
on the FTF. The purpose of this study was to determine if these two codes could
be used for the successful prediction of the FTF aerodynamic parameters. To make
this determination, the instrumented FTF was attached to the underside of an F-104G
aircraft and flight data were obtained. At Mach 0.6, 0.7, 0.8, 0.85, and 0.9,

pressure distributions and boundary-layer displacement thicknesses were determined from the flight test data and were compared with the predicted values obtained using code H. Pressure distributions between Mach 0.6 and 1.4 were made and compared to those predicted using the wing-body code.

NOMENCLATURE

C_p pressure coefficent, $\dfrac{p - P_\infty}{\bar{q}}$

c   local streamwise chord of wing panel, cm (in)

FTF   flight test fixture

p   static pressure, N/m^2 (lb/ft^2)

P_∞ free-stream static pressure, N/m^2 (lb/ft^2)

$\bar{q}$ free-stream dynamic pressure, $0.7M^2 P_\infty$, N/m^2 (lb/ft^2)

Re   Reynolds number

x   chordwise distance from leading edge, positive aft, cm (in)

x/c   ratio of distance from leading edge to local chord length

y   spanwise distance from bottom of FTF, positive up, cm (in)

α   angle of attack, deg

δ^* boundary-layer displacement thickness, cm

DESCRIPTION

Flight Test Fixture

The FTF had a low-aspect-ratio, fin-like shape and was mounted on the underside of an F-104G aircraft. The longitudinal axis was aligned on the aircraft lower fuselage centerline (fig. 1). The FTF (fig. 2) was made primarily of aluminum and weighed approximately 136 kg (300 lb), had a chord length of 203.20 cm (80.0 in), a span of 60.96 cm (24.0 in), and a constant thickness of 16.20 cm (6.4 in) except for the forebody. Two options were available for forebody shapes: (1) the basic FTF shape with a sharp leading edge (wedged forebody), and (2) the radiused forebody incorporating the front portion of a symmetric supercritical airfoil. Only the wedged forebody was used in this study. The fin air data system consisted of a pitot static probe mounted on a boom and extending forward from the FTF. The probe was used to measure Mach number, altitude, and dynamic pressure.

The FTF was equipped with flush static-pressure orifices for measurements of chordwise and spanwise pressure distributions, and boundary-layer rakes for measurement of the boundary-layer velocity profile. For this study, 20 static orifices were located on each side of the FTF (fig. 3). Sixteen orifices were placed along the chord at approximately the 50-percent span position. Four orifices were located along a spanwise direction to determine spanwise flow conditions. The boundary-layer rakes were mounted on both sides of the FTF at approximately the 90-percent chord and 50-percent semispan positions. The FTF is described in more detail in reference 3.

A pulse-code modulation system was used for data acquisition. Data from this system, which is capable of multiplexing 40 channels at a maximum frequency of 80 Hz, were telemetered to the ground computer and recorded onboard the aircraft. All pressure measurements were obtained by a 48-port pressure-scanning valve and two differential pressure transducers. These pressure measurements were referenced to the static pressure measured by the FTF boom.

Aircraft

The F-104G aircraft has an independent instrumentation system and an aircraft flight trajectory guidance system. Engineering parameters calculated on a ground-based computer are uplinked in real time to a cockpit display through the trajectory guidance system. From this display, the pilot can obtain real-time determination of errors in Mach number, Reynolds number, and sideslip, as well as bank-angle error during constant Mach, angle-of attack, and altitude turns.

Code H Analysis

Bauer and his associates at the Courant Institute of Mathematical Sciences of New York University developed a technique of computing supercritical airfoil sections and determining the off-design flow conditions (ref. 1). The equations of motion used in this method are the equations of potential flow. The flow is assumed to be transonic, steady, irrotational, inviscid, compressible, and two-dimensional.

Instead of solving the problem of computing shock-free transonic flow over a given profile, the inverse problem is solved. That is, a smooth transonic flow is assumed and the body that generated it is ascertained. This approach is taken to eliminate certain mathematical difficulties. The problem is formulated by writing the equations of motion of the inverse problem in matrix form, extending all variables into the complex domain, introducing characteristic coordinates, and then expressing the equations of motion in characteristic form. A treatment of compressibility is made by combining a general solution with a singular solution related to the fundamental solution in the hodographic plane. The formulated equations are solved numerically using a finite-difference scheme. Hence, the shape that would result in the smooth transonic flow is determined by this inverse method, and the off-design flow conditions (at different angles of attack and free-stream velocities) are also solved.

Bauer and his associates modified and improved their original work by introducing a better model of the trailing edge and using a rotated finite-difference scheme that enabled the use of an arbitrary curvilinear coordinate system. Such a coordinate system permits the handling of supersonic and subsonic free-stream Mach numbers and the capturing of shock waves as far aft on the airfoil as desired. The turbulent boundary layer is treated using a semiempirical method, and the effects of displacement thickness on airfoil shape are included. Shock waves are calculated with weak solutions to the applicable partial differential equations that include one or more shock waves satisfying an entropy inequality. These modifications are included in a new program designated code H (ref. 1). These programs are claimed to provide a physically adequate computer simulation of the compressible potential problems of transonic flow for a smooth two-dimensional shape.

Wing-Body Code Analysis

The Boeing Company, under contract with NASA Ames Research Center, has developed a three-dimensional wing-body constant-pressure panel code for subsonic and supersonic potential flows. The program calculates steady pressure distributions on wing and wing-body combinations of arbitrary planform in subsonic and supersonic flow. The surface pressures are integrated to give lift, drag, and pitching moment. The yawing and rolling moments and the side force can be determined for asymmetric configurations; however, for this study, only the pressure coefficients predicted for the FTF surface were used. In addition, the original version of the Ames wing-body code was modified by personnel at Ames, and an updated version of this program was made available to Ames-Dryden for this study.

The method divides the wing only or the wing-body combination into numerous constant-pressure panels. A constant-source distribution is used in the body panels, and a vortex distribution is used in the wing and tail panels. Analytical expressions are obtained for the perturbation velocities induced at each panel. The pressure coefficient at the panel control points are then calculated in terms of the perturbation velocities. The forces and moments acting on the wing-body combination can be calculated by using a numeric integrating scheme.

A further description, as well as previous application of the wing-body code at Ames-Dryden, is given in reference 4.

MODELING OF FLIGHT TEST FIXTURE

Code H Modeling

In all cases presented, the code was operated for 0° angle of attack, and four smoothing iterations of the FTF coordinates were made before the aerodynamic shape was conformly mapped into the unit circle. The circle was overlaid with both a coarse grid of 80- by 15-mesh intervals and a finer grid of 160- by 30-mesh intervals in the angular and radial directions. Flow calculations and boundary-layer corrections were computed for a maximum of 20 cycles on the coarse grid, and a maximum of 10 cycles on the finer grid. The convergence tolerance, a tolerance of the

maximum velocity potential and the maximum circulation corrections, was set at $\pm 5 \times 10^{-6}$. The program was operated until the convergence tolerance was achieved. The boundary-layer correction option of the code was used, and the transition was set at the 7.5-percent chord position. To utilize this option, a Reynolds number Re must also be specified. In this case, $Re = 2 \times 10^6$ and 14×10^6 were used.

The FTF was first modeled using 46 upper and 46 lower surface points with a high density of points at the wedge corner of the FTF located approximately at the 17-percent chord position. Because of the discontinuity at the corners, the code H operation could not be completed. A model with 46 upper and 46 lower surface points was again attempted. This time, however, the sharp corners of the wedge were radiused and the coordinates were run through a separate smoothing program before being entered into the two-dimensional code. Figure 4 shows a comparison of this model shape with the actual FTF shape. A comparison of the predicted and experimental pressure distributions for Mach 0.7 is shown in figure 5. The code-predicted pressure distribution appears to determine the pressure coefficient levels well; however, the peak values of pressure coefficients differ at approximately 7-percent chord in the chordwise location. In addition, the experimental data indicate a trend of decreasing pressure at the FTF trailing edge that is not predicted by the code. The variations in the peak pressure coefficient positions between the experimental and the computer-predicted data (fig. 5) were believed to be caused by the differences in the shape of the actual and the computer models.

To test this hypothesis, the code H program was operated with a model consisting of 16 upper and 16 lower surface points. This model with fewer points allowed the smoothing subroutine internal to the code to have a greater effect (fig. 6). The shape of the model is very similar to the actual FTF. Figure 7 shows good correspondence for the positions of the minimum pressure coefficients determined from experimental and theoretical data. The noted lack of correlation of pressure coefficients at the trailing edge was not believed to be caused by modeling and is discussed in the RESULTS section of this report.

Wing-Body Code Modeling

Because the wing-body code is three-dimensional, the F-104G aircraft as well as the FTF had to be modeled. The wing-body code allows for a maximum of 100 wing and 100 body panels. These panels were divided among the F-104G fuselage and wing and the FTF. The fuselage was modeled with 96 panels; 32 panels were used for the F-104G wings, and 50 panels for the FTF (fig. 8). The F-104G fuselage was modeled as a cylinder with an 80.00 cm (31.5-in) radius, an 1160.00-cm (456.7-in) length, and a 470.00-cm- (185.0-in-) long conical nose. The F-104G wings were modeled as a biconvex surface with a 3.36-percent thickness ratio, a 230.00-cm (90.5-in) semi-span length, an 18.60° back sweep of the quarter chord, and a 10° anhedral. To allow more panels for the FTF, the vertical and horizontal stabilizers were not included in the model.

Code H Pressure Distributions

The FTF pressure distributions were calculated from experimental and theoretical data for Mach 0.7, 0.8, 0.85, and 0.9, as shown in figures 9(a) to 9(d). The experimental data were based on Mach numbers measured with the FTF nose boom as only the FTF was modeled in this case. Code H was used to calculate the theoretically determined pressure coefficients. As shown in figure 9(a), at Mach 0.7, the flow accelerated and the pressure coefficient dropped from the leading edge of the FTF to the point on the FTF where the discontinuity occurred (approximately 17-percent chord). Beyond this point, the flow slowed as it changed direction and the pressure coefficient increased. With the exception of the peak minimum values of pressure coefficients, the experimental data correlated well with the theoretical data. Code H predicted higher minimum pressure coefficients than were obtained from the flight test data. No shock existed for Mach 0.7, as supersonic flow velocities did not occur on the FTF.

For Mach 0.8, 0.85, and 0.9, the flow accelerated from the nose to the surface discontinuity and reached a sonic condition, as indicated in figures 9(b) to 9(d). As the flow turned through an angle of approximately 13.05° (one-half of the wedge angle) at the discontinuity point, it accelerated to a peak value and went through a normal shock. The shock caused a rapid increase in the pressure coefficient and a slowing of the flow to subsonic velocities. Figures 9(b) to 9(d) reveal a fairly good correspondence between the experimental and theoretical data. However, the peak minimum values of pressure coefficients differed, and as the Mach number increased from 0.8 to 0.85, the predicted shock location tended to shift beyond the 20-percent chord position. For the theoretical data, the shock at Mach 0.9 shifted to about the 50-percent chord position. The shock remained near the 20-percent chord position for all Mach numbers for the experimental data. Hence, code H does not accurately predict shock location for the wedge-shaped test fixture near Mach 1 or at high transonic speeds.

At approximately the 70-percent chord position on the FTF, the two curves diverged and the experimental data revealed a decreasing pressure that was not predicted by the theoretical method. The disparity between these two curves may be explained as follows. The FTF can be considered to be an aft-facing step with a height equal to one-half the fixture width; flight-measured pressure characteristics of the aft-facing steps presented in reference 5 indicate that the base pressure does affect the pressure measured upstream of the aft-facing step. However, the code does not account for this because a trailing edge of finite thickness is advanced linearly until it closes or exceeds chord length, whichever occurs first. An attempt was therefore made to alter the trailing edge of the FTF model. The model was geometrically scaled down, and a boattail was added to effectively accelerate the flow at points near the trailing edge.

The pressure distribution for the boattail FTF in figure 10 shows that decreasing pressure at the trailing edge was evident but was insufficient to match the experimental data. A boattail of greater curvature was attempted, but the code

would not operate as points spaced too closely together at the trailing edge caused computational difficulties. Even with fewer points at the trailing edge, a code operation could not be completed because more curvature was needed to simulate the flow at the trailing edge.

Wing-Body Pressure Distributions

The wing-body code was operated for the combined F-104G fuselage and wing and the FTF model at Mach 0.6, 0.7, 0.8, 0.9, 1.2, and 1.4. Angles of attack of 0°, 2°, and 4° were used for the two extreme cases of the Mach number range, Mach 0.6 and 1.4. These two cases were operated at different angles of attack to determine the effects of aircraft angle of attack on the data. Figures 11(a) and 11(f) show both the theoretical wing-body code data and the experimental flight test data for these two cases. Little difference existed for the three sets of angle-of-attack data. Hence, for Mach 0.7, 0.8, 0.9, and 1.2, the code was operated at 2° angle of attack, which approximates the F-104G angle of attack during the test flights. The code was operated for all Mach numbers at 0° sideslip angle, and the flight test data were recorded at sideslip angles of ±0.5°. The pressure coefficients given in the output of the wing-body code acted at the centroid of the panel and represented the average pressure over the panel. Because the wing-body code is three-dimensional and the model included the aircraft, the flight test data were based on Mach numbers measured by the aircraft instrumentation system rather than the FTF air data system.

Figures 11(a) and 11(b) depict data for Mach 0.6 and 0.7. These data indicate an accelerating flow from the FTF nose to the surface discontinuity and a decelerating flow aft of the FTF forebody with an accompanying increase in pressure coefficient. The flight test data correlated fairly well with the theoretically predicted data. The peak negative pressure coefficient for the flight test data was more negative than the predicted value; the predicted values of pressure coefficent were generally higher than the flight-measured data. As was the case for code H, the trend of decreasing pressure coefficients near the FTF trailing edge indicated in the flight test data was not indicated in the theoretically predicted data.

Figures 11(c) and 11(d) show data for Mach 0.8 and 0.9. At these flight speeds, the flow was accelerated over the FTF forebody to supersonic speeds, and a normal shock wave formed. These shock waves were evident in the flight test data for Mach 0.8 and 0.9. While the shock waves were not predicted by the wing-body code, the point of minimum pressure coefficient did occur at the 20-percent chord position for both sets of data. The wing-body code is not capable of transonic shock wave prediction. Again, the data indicated an inability of this code to predict the decreasing values of pressure coefficient near the FTF trailing edge for similar reasons as code H results. However, for Mach 0.9, the two sets of data correspond very well over a wide range of chord positions.

The data for the Mach 1.2 and 1.4 cases are shown in figures 11(e) and 11(f). For both cases, the flow over the FTF was subsonic because 13.05° (one-half of the wedge angle) was large enough to cause the shock to detach from the FTF nose. The portion of the shock forward of the nose was normal, and the normal shock wave created a subsonic flow over the FTF nose and large, positive pressure coefficients.

The flow accelerated over the forebody did not reach sonic conditions and decelerated from the surface discontinuity to the trailing edge. The two sets of data matched very well over the entire FTF. However, in the Mach 1.2 case, the theoretical data reflected very sharp changes in pressure coefficient about the 50-percent chord position. The wing-body code may have introduced fuselage effects that did not occur in the experimental data at this particular Mach number. To check this possibility, the FTF was modeled excluding the F-104G aircraft.

Figure 12 shows that the pressure distribution smooths out and compares well to the experimental data, suggesting that the code was indeed introducing inaccurate fuselage effects. The trailing edge divergence noted in the subsonic data changed for the supersonic data. The experimental data indicate an increasing and then decreasing trend of pressure coefficients near the FTF trailing edge.

Displacement Thickness Distribution

Code H provides a semiempirical turbulent boundary-layer correction in the transonic flow analysis. The boundary-layer displacement thickness is calculated by relating momentum thickness and shape factor where momentum thickness is determined using Von Kármán's equation and the shape factor is determined semiempirically. Because the laminar portion of the boundary layer is considerably smaller than the turbulent portion, it is not considered in the boundary-layer correction calculations. For the boundary-layer correction, a transition point must be specified. A transition location of 7.5-percent chord was used in all cases. This most closely approximated where transition was thought to occur.

In figure 13, experimental and theoretical displacement thickness at 85-percent chord are plotted with Mach number. Reynolds numbers of $Re = 2 \times 10^6$ and 14×10^6 were used for the theoretical data. The shapes of the curve agree but are displaced. Also, the experimental data for $Re = 20 \times 10^6$ were quite scattered near Mach 0.8. This scatter was probably caused in part by separated flow due to a shock wave that was reattaching. It was concluded from the data in figure 13 that the semiempirical boundary layer used in code H does not permit precise determination of the displacement thickness for the FTF with the wedge-shaped nose.

CONCLUSIONS

An F-104G aircraft with an attached flight test fixture (FTF) with a wedge-shaped forebody was tested at the Dryden Flight Research Facility of NASA Ames Research Center. Pressure distributions and displacement thicknesses were determined from the flight test data. Two theoretical prediction methods were used to predict similar data for the FTF at the flight test speeds. One is a two-dimensional method and has been designated code H by Bauer and his associates, the authors of this method. The other is a three-dimensional method and has been designated as the wing-body code by its author, Frank Woodward. The comparisons of

8

experimental flight test data with the theoretical data predicted by the codes may be summarized as follows:

1. For subsonic flight speeds and flow over the FTF, code H adequately predicts values of pressure coefficients except at the minimum pressure point and at the trailing edge. Code H predicts higher values at the minimum pressure point, and the experimental data reveal a decreasing pressure coefficient that code H does not predict.

2. For subsonic flight speeds and supersonic flow at some point on the FTF, the shock wave that forms is located at the approximately 20-percent chord position. Code H predicts a shifting position of the shock waves with increasing speed and does not adequately predict the decreasing pressure coefficient divergence at the FTF trailing edge. However, code H adequately predicts the level of the pressure coefficients at other positions on the FTF.

3. For subsonic speeds and flow over the FTF, the wing-body code adequately predicts levels of pressure coefficients except at the trailing edge. The decreasing pressure coefficient divergence at the trailing edge is not predicted by the wing-body code.

4. The wing-body code is incapable of predicting shock waves. However, for subsonic flight and supersonic flow at some point on the FTF, the code adequately predicts pressure coefficient levels except at the trailing edge and the minimum pressure point.

5. For supersonic flight speeds and subsonic flow over the FTF, the wing-body code adequately predicts levels of pressure coefficients.

6. The semiempirical boundary layer used in code H does not precisely predict the displacement thickness of the FTF for the two Reynolds numbers tested (Re = 2×10^6 and 14×10^6).

National Aeronautics and Space Administration
Ames Research Center
Dryden Flight Research Facility
Edwards, California, November 22, 1985

9

REFERENCES

1. Bauer, Frances; Garabedian, Paul R.; Korn, David; and Jameson, Antony:
   Supercritical Wing Sections II, Control Theory No. 108. Lecture Notes
   in Economics and Mathematical Systems, M. Beckmann and H.P. Künzi, eds.,
   Springer-Verlag, New York, 1975.

2. Woodward, Frank A.: Analysis and Design of Wing-Body Combinations at
   Subsonic and Supersonic Speeds. J. Aircraft, vol. 5, no. 6, Nov.-Dec.
   1968, pp. 528-534.

3. Meyer, Robert R., Jr.: A Unique Flight Test Facility: Description and
   Results. NASA TM-84900, 1982.

4. Curry, Robert E.: Utilization of the Wing-Body Aerodynamic Analysis Program.
   NASA TM-72856, 1978.

5. Powers, Sheryll Goecke: Flight-Measured Pressure Characteristics of Aft-Facing
   Steps in Thick Boundary Layer Flow for Transonic and Supersonic Mach Numbers.
   YF-12 Experiments Symposium, NASA CP-2054, vol. I, 1978, pp. 201-226.

ECN 18005

*Figure 1. Flight test fixture installed on lower fuselage of
F-104 carrier aircraft.*

34.93 cm
(13.8 in)

203.20 cm
(80.0 in)

16.20 cm
(6.4 in)

45.72 cm
(18.0 in)

60.96 cm
(24.0 in)

52.83 cm
(20.8 in)

3°
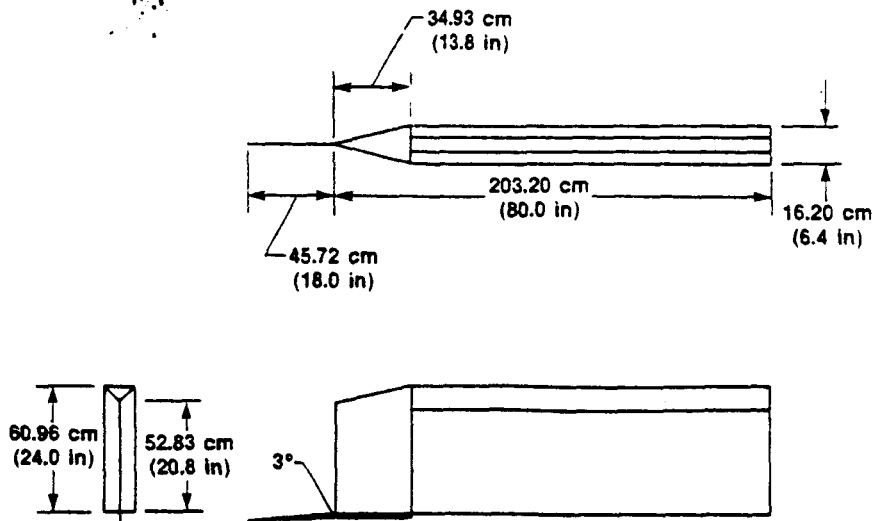
Figure 2. Three-view drawing of flight test fixture.

x

20
19
12
11 13
18
17

1 2 3 4   5   6   7   8   9   10   11   13   14   15   16

26.92 cm
(16.0 in)

y
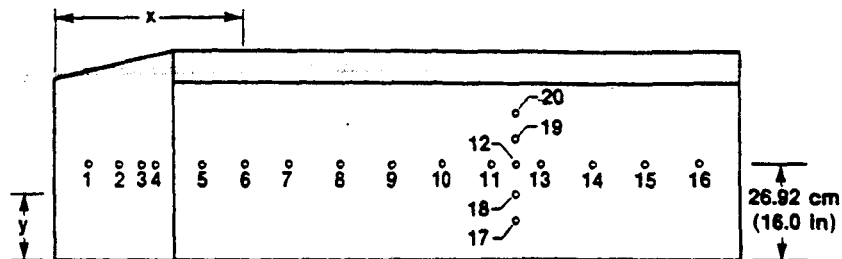
Orifice	x, cm (in)	Orifice	x, cm (in)	Orifice	y, cm (in)
1	9.53 (3.75)	9	99.06 (39.00)	17	11.68 (4.60)
2	19.05 (7.50)	10	114.30 (45.00)	18	19.30 (7.60)
3	24.90 (9.80)	11	129.54 (51.00)	19	34.29 (13.50)
4	29.21 (11.50)	12	137.16 (54.00)	20	41.91 (16.50)
5	43.18 (17.00)	13	144.78 (57.00)		
6	55.88 (22.00)	14	160.02 (63.00)		
7	68.58 (27.00)	15	175.26 (69.00)		
8	83.82 (33.00)	16	190.50 (75.00)		

Orifice 3 is on right side only; orifices
1, 2, and 4 are on right and left sides

Figure 3. Orifice locations for flight test fixture.

Figure 5. *Pressure distribution gener-
ated by code H for 92-point model of
flight test fixture, Mach 0.7.*

*Figure 4. Comparison of radiused-nose
model shape to actual shape of flight
test fixture.*
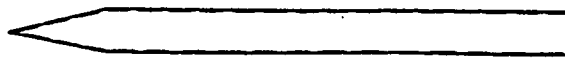
*Figure 6. Comparison of 32-point
model to actual shape of flight
test fixture.*
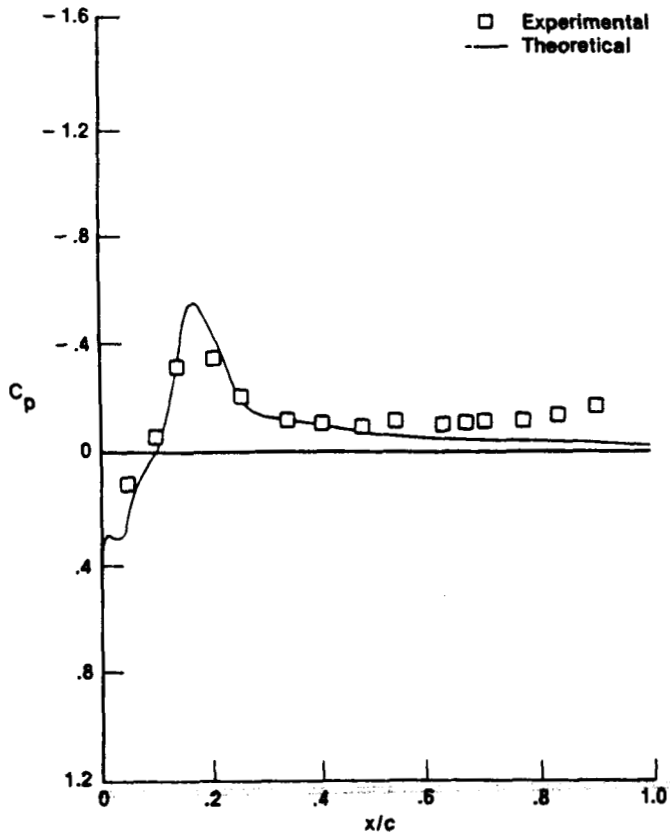
Figure 7. Pressure distribution gener-
ated by code H for 32-point model of
flight test fixture, Mach 0.6.
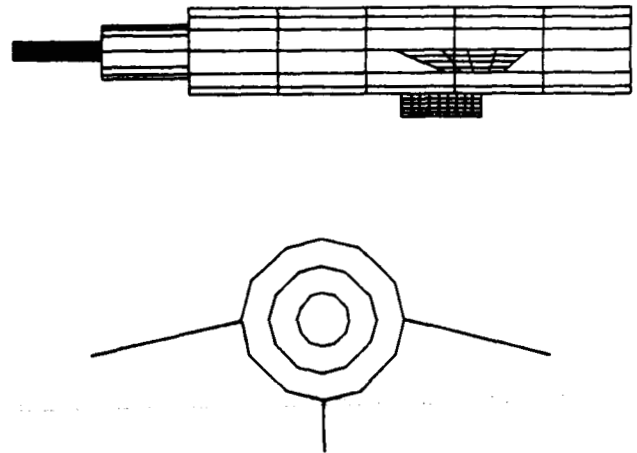
Figure 8. Panel detail of F-104 flight
test fixture model used for wing-body
code.
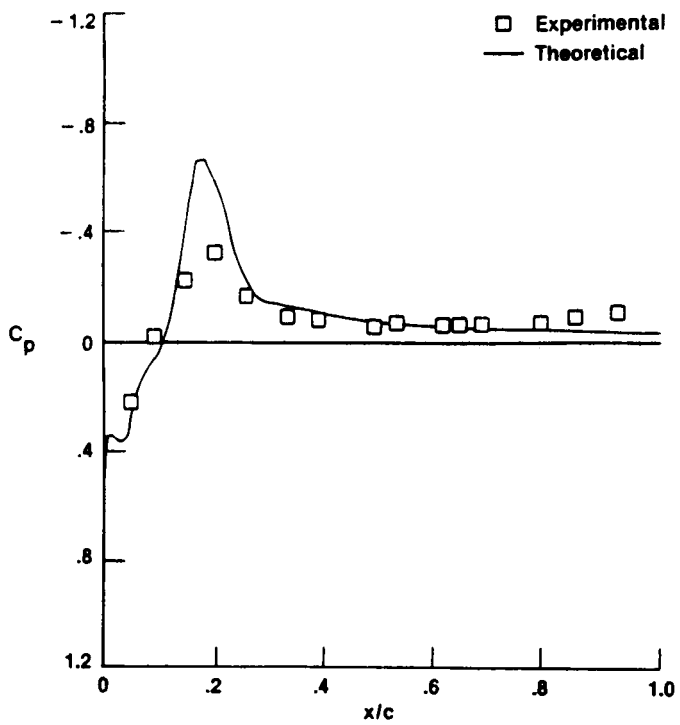
(a) Mach 0.7.
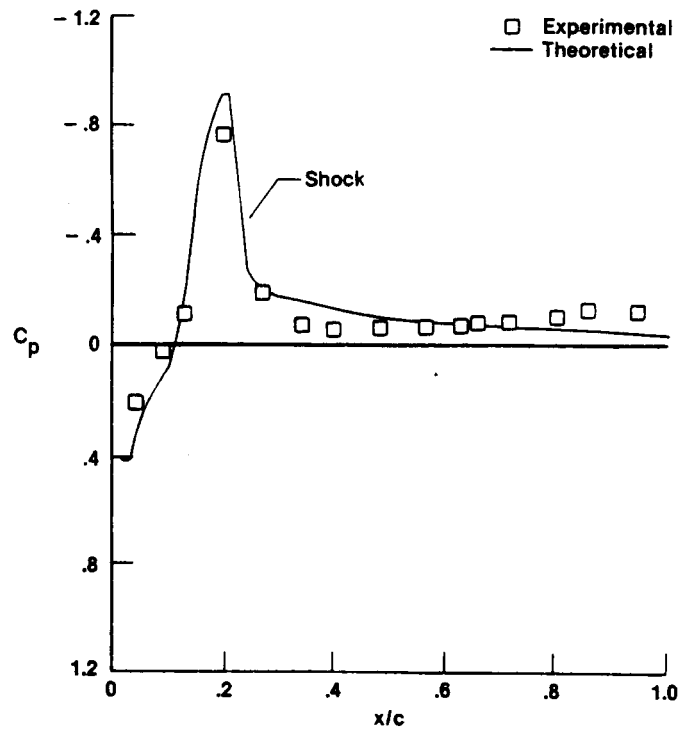
(b) Mach 0.8.
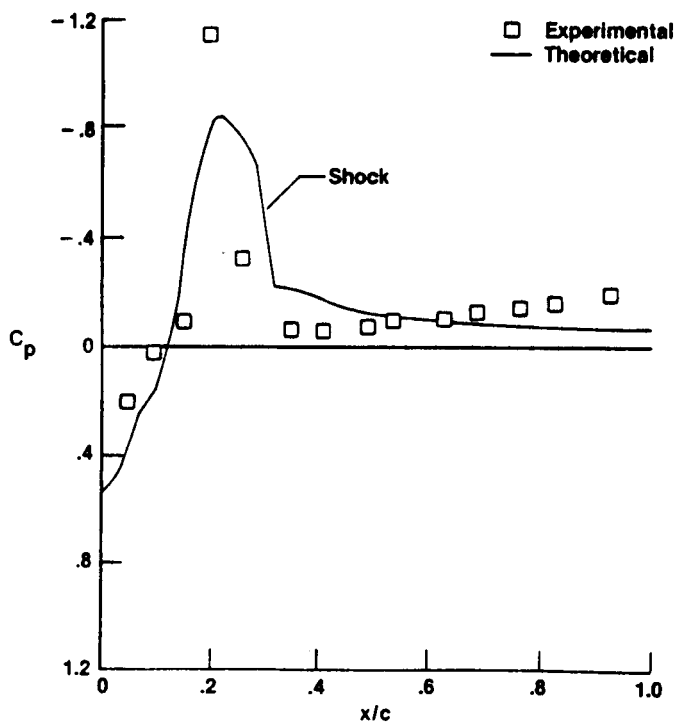
(c) Mach 0.85.
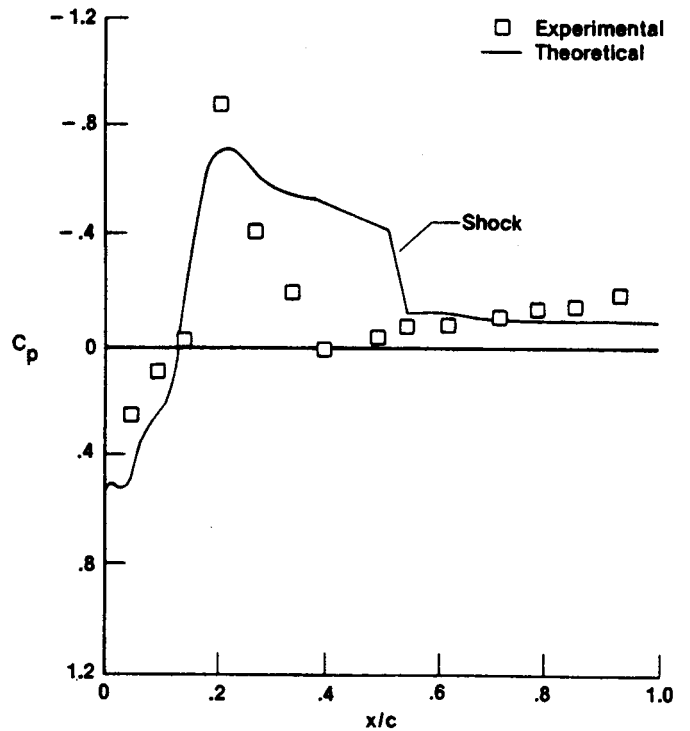
(d) Mach 0.9.

Figure 9. Pressure distribution generated using code H.
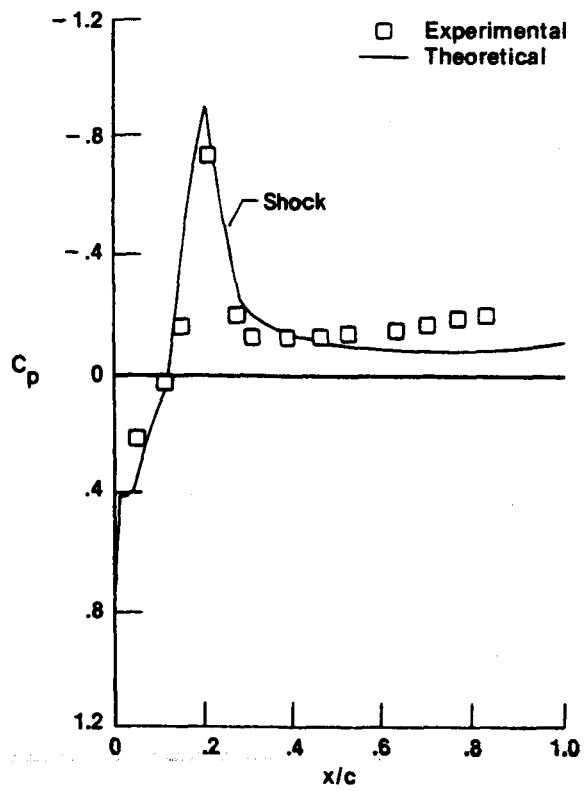
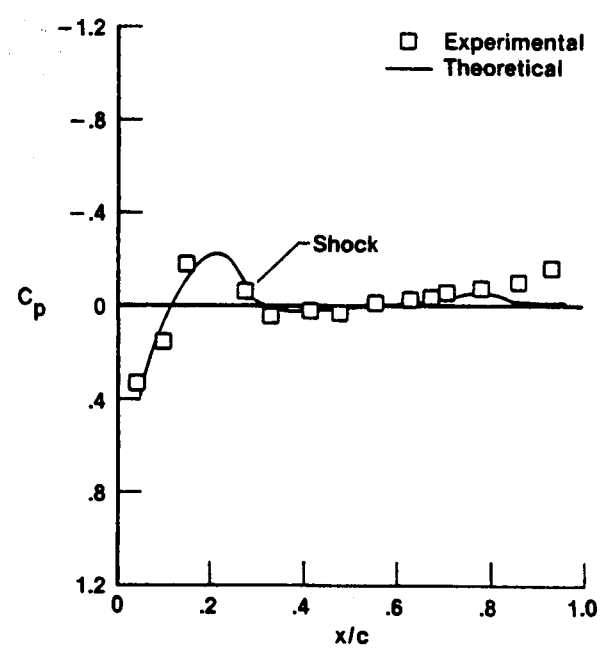*Figure 10. Pressure distribution generated by code H for boattail model of flight test fixture, Mach 0.8.*
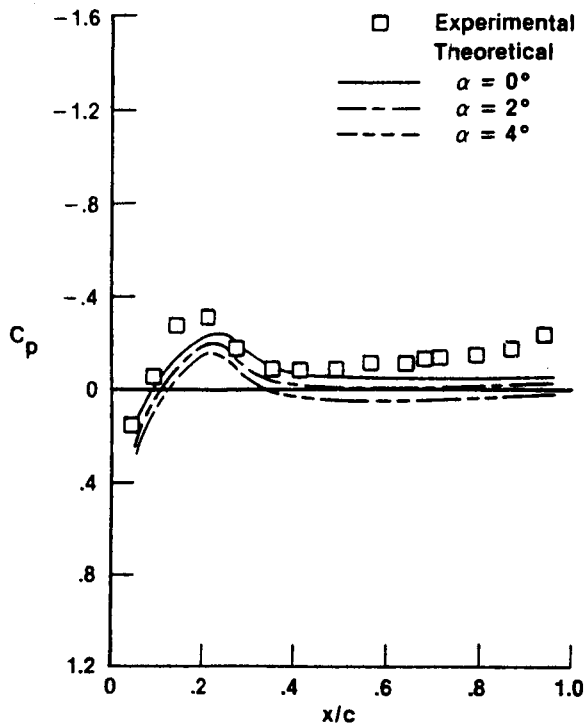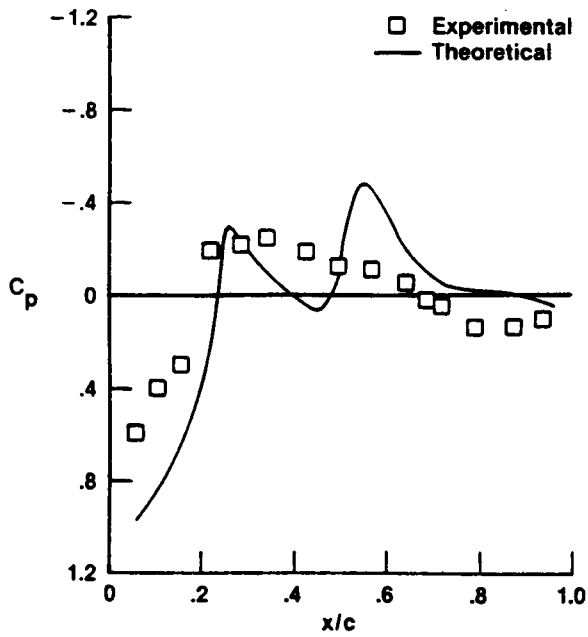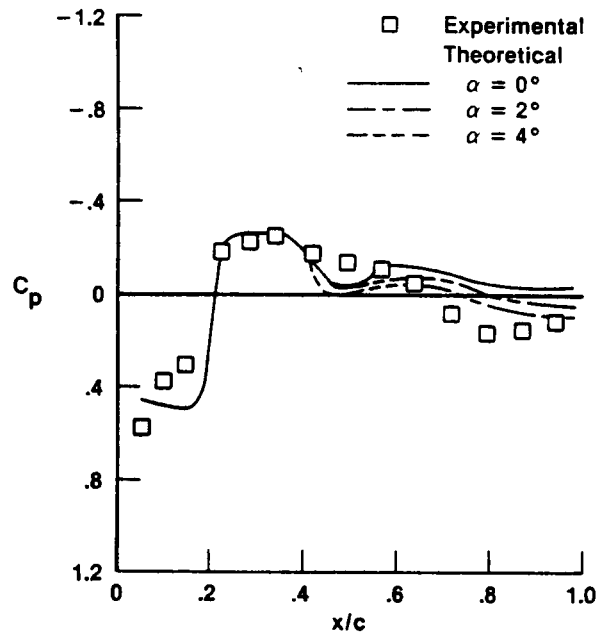
(a) Mach 0.6.
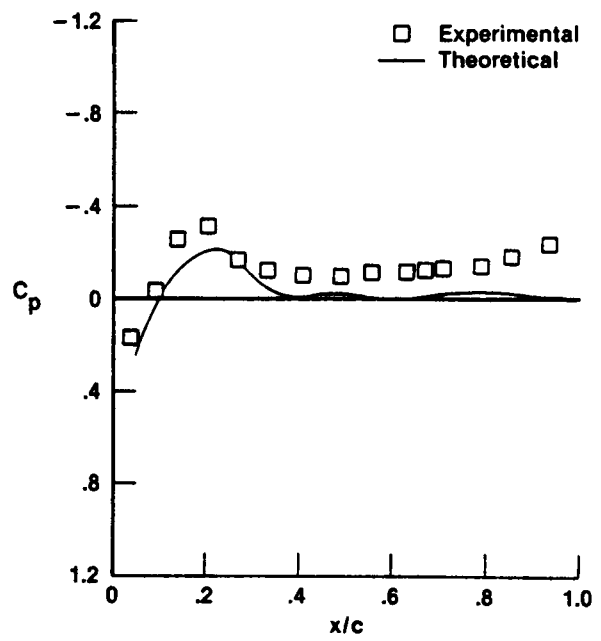
(b) Mach 0.7.
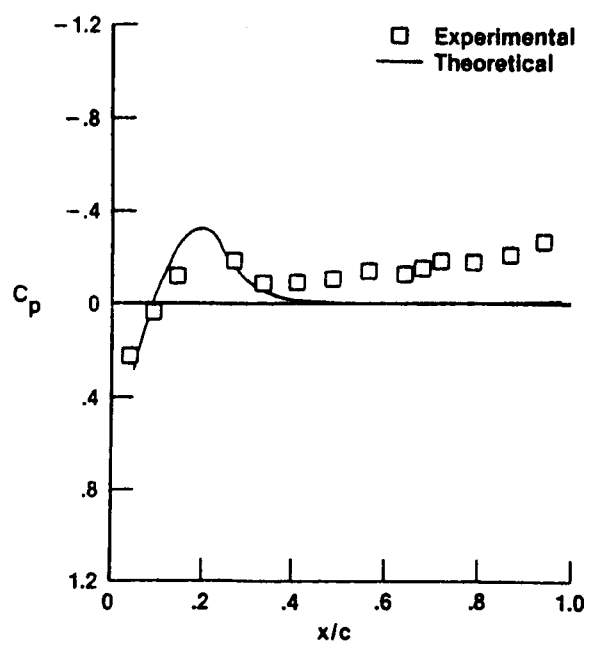
(c) Mach 0.8.

(d) Mach 0.9.

Figure 11. Pressure distribution generated by wing-body code.

(e)   Mach 1.2.

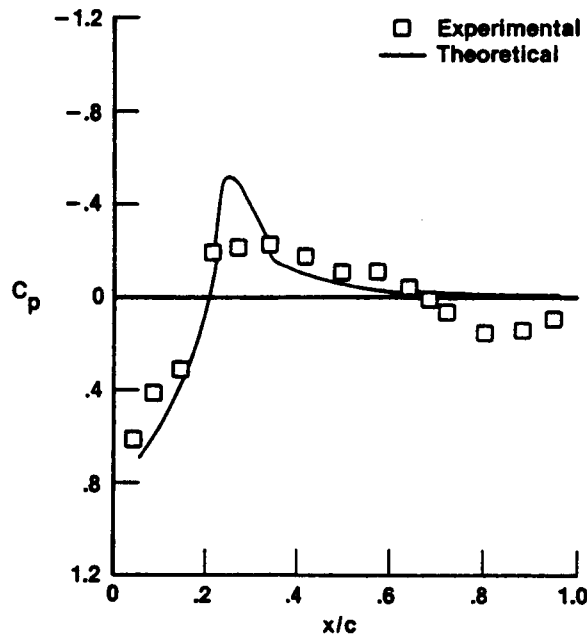(f)   Mach 1.4.

Figure 11. *Concluded.*

Figure 12. *Pressure distribution generated by wing-body code for isolated flight test fixture model.*
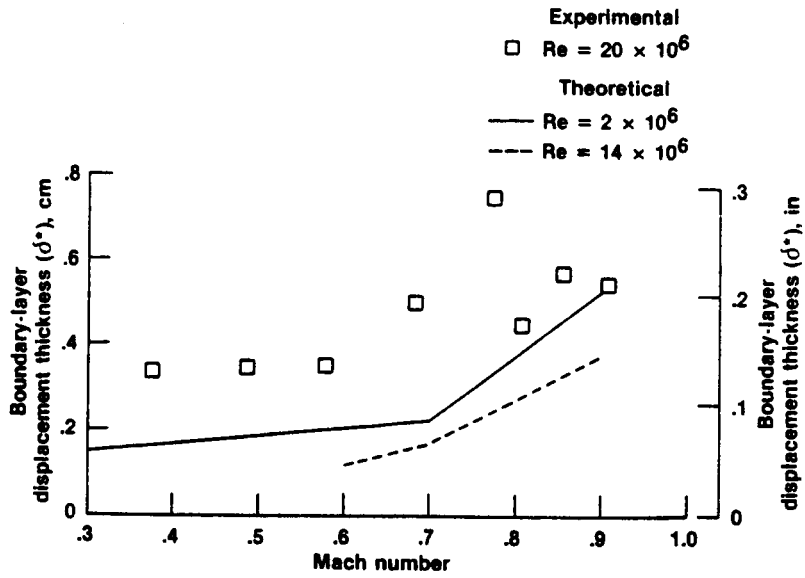
Figure 13. Displacement thickness generated by code H as a function of Mach number.

1. Report No. NASA TM-86806	2. Government Accession No.	3. Recipient's Catalog No.
4. Title and Subtitle Comparison of Theoretical and Flight-Measured Local Flow Aerodynamics for a Low-Aspect-Ratio Fin		5. Report Date December 1986
		6. Performing Organization Code
7. Author(s) J. Blair Johnson and Doral R. Sandlin		8. Performing Organization Report No. H-1336
		10. Work Unit No. RTOP 505-60-21
9. Performing Organization Name and Address NASA Ames Research Center Dryden Flight Research Facility P.O. Box 273 Edwards, CA 93523-5000		11. Contract or Grant No.
		13. Type of Report and Period Covered Technical Memorandum
12. Sponsoring Agency Name and Address National Aeronautics and Space Administration Washington, DC 20546		14. Sponsoring Agency Code

16. Abstract

Flight test and theoretical aerodynamic data were obtained for a flight test fixture mounted on the underside of an F-104G aircraft. The theoretical data were generated using two codes: (1) a two-dimensional transonic code called code H, and (2) a three-dimensional subsonic and supersonic code called wing-body. Pressure distributions generated by the codes for the flight test fixture, as well as boundary-layer displacement thickness generated by the two-dimensional code, were compared with the flight-measured data. The two-dimensional code pressure distributions compared well except at the minimum pressure point and the trailing edge. Shock locations compared well except at high transonic speeds. However, the two-dimensional code did not adequately predict the displacement thickness of the flight test fixture. The three-dimensional code pressure distributions compared well except at the trailing edge of the flight test fixture.

17. Key Words (Suggested by Author(s)) Experimental flight data Pressure distribution Wedge-shaped airfoil	18. Distribution Statement Unclassified — Unlimited Subject category 02

19. Security Classif. (of this report) Unclassified	20. Security Classif. (of this page) Unclassified	21. No. of Pages 19	22. Price* A02